Scan-angle-independent FEM Analysis of Infinite Arrays based on Spherical Harmonic Lattice Sums and the Generalized Scattering Matrix of an Isolated Antenna

Jesús Rubio, Miguel Á. González de Aza, Juan Córcoles, *Senior Member IEEE*, and Rafael Gómez Alcalá, *Member, IEEE*

***Abstract*— Infinite periodic arrays of antennas that can be individually described by means of spherical modes are analyzed starting from the Generalized Scattering Matrix (GSM) of an isolated element. After computing the Generalized Scattering Matrix of an isolated element with the Finite Element Method, a fast post-processing can be carried out to calculate the response of the element in an infinite array environment by using addition theorems for spherical modes. For this purpose, an efficient computation of lattice sums of spherical harmonics is used. The main advantage of this method is that the antenna is analyzed only once whatever the array lattice or scan angle. Additionally, fast frequency analysis can be performed since the starting point is the computation of the isolated antenna with the Finite Element Method, which is suitable for fast frequency sweep. The active reflection coefficient and the embedded radiation pattern of the infinite periodic array are calculated for several examples to show the capabilities of the proposed method.**

***Index Terms*— Spherical Modes, Addition Theorems, Finite Element Method, Lattice Sums, Generalized Scattering Matrix.**

I. Introduction

Research on infinite arrays made up of periodically arranged antennas has been carried out for a long time since it constitutes the core model for the analysis and design of large phased antenna arrays [1], [2]. The importance of the infinite array model as a pre-design tool is confirmed by the fact that the main commercial software incorporates it [3]-[5]. Although a great effort has been made in recent years for the efficient analysis of finite arrays [6], for example, using spherical mode expansion [7] or far-field data and iterative methods [8], their use in the design of periodic arrays of hundreds or even thousands of elements requires computational times that are too high for design purposes. In those cases, infinite array analysis is still preferred. The main advantage of the infinite array model is that, because of Floquet theorem [9], only a single antenna element, i.e. unit cell of the antenna array, needs to be analyzed through the application of proper periodic Floquet boundary conditions and modal expansions [2]. Once results from this unit cell are computed, the behavior of a finite phased array can be readily estimated on the basic assumption that it is large enough, so that central antenna elements dominate this behavior [2].

In the last decades, a number of computational methods to enable accurate simulations of infinite periodic arrays have been proposed (see, for example, the thorough review in the introduction of [10]). This variety, together with the technological developments in phased antenna arrays, can make the designer choose the most appropriate method according to the phased array structure and materials. As said, the application of Floquet theorem [9] is a shared common ground for all these methods to compute a Generalized Scattering or a Generalized Admittance Matrix in terms of Floquet modes [11]-[15]. Among these methods, the Finite Element Method (FEM), both in the time and the frequency domain [16], has turned out to be quite popular because of its capability to model complex materials and structures.

The analysis of infinite periodic arrays with the frequency-domain three-dimensional (3D) FEM has been long known since it was proposed in the mid-1990's [17]-[19]. In spite of its popularity, the 3D-FEM analysis of infinite periodic structures based on Floquet theory still suffers from three major issues: 1) the application of periodic boundary conditions onto opposite faces of the unit cell may not be straightforward for non-matching meshes; thus, matching meshes are desirable, but the generation of such meshes incurs in complicated meshing procedures and it is sometimes infeasible for complicated structures; 2) a different FEM simulation of the unit cell is required for each scan angle of the infinite phased array, as the desired scan angle changes both the Floquet modes and the shift in periodic boundary conditions to be applied; thus, a complete

Manuscript received February 22, 2022; revised June 10, 2022; accepted July 5, 2022. This work was parcially supported by Ministerio de Ciencia e Innovación (MCIN/AEI /10.13039/501100011033 / FEDER, UE) under projects PID2021-122856NB-C21 and PID2021-122856NB-C22, and by Junta de Extremadura /European Regional Development Funds, EU, under project GR21072.

J. Rubio and R. Gómez Alcalá are with Escuela Politécnica, Universidad de Extremadura, Avda. de la Universidad, s/n 10003 Cáceres, Spain. (E-mails: jesusrubio@unex.es and rgomezal@unex.es).

M.A.González de Aza is with with the Information Processing and Telecommunications Center, Universidad Politécnica de Madrid (UPM), 28040 Madrid, Spain. (E-mail: mag@etc.upm.es).

J. Córcoles is with Escuela Politécnica Superior, Universidad Autónoma de Madrid, 28049 Madrid, Spain. (E-mail: juan.corcoles@uam.es).

characterization (i.e. embedded element pattern or active reflection coefficient per scan angle) requires several full-wave simulations (in a discretized scan angle range); and 3) there is a need to know *a priori* the regular arrangement (the *lattice*) of the antennas in the array (i.e., shape and dimensions of the unit cell) since, again, the shift in periodic boundary conditions and the Floquet modes depend on this; though this can be regarded as obvious, in the end a degree of freedom in the design process is subtracted as a different lattice would entail a new full-wave FEM simulation per scan angle. After the mentioned seminal works [17]-[19], later works focused on addressing the issue of matching face triangulations, either using prismatic elements [20], or by directly proposing FEM strategies for non-matching meshes [21],[22],[15].

To the best of the authors' knowledge, [23] is the only work reporting a FEM analysis independent of the scan angle, valid for aperture-type antennas. It is based on the matching of FEM basis functions and the Floquet modes in the aperture, although special care should be taken to avoid convergence issues in this matching procedure.

To reduce the computational effort due to the need to carry out one unit cell FEM analysis for each scan angle, some commercial software such as HFSS/ANSYS have developed efficient interpolation methods in one of the angular directions for a fixed value of the other one. However, this approximation may still require up to 15 FEM analyses for each fixed angular direction for an error lower than 0.01 in S parameters [24].

In this work, we propose a full-wave strategy based on 3D-FEM for the characterization of infinite arrays of antennas that can be individually described in terms of spherical modes. The proposed method overcomes, for this type of antennas, the aforementioned current three major issues regarding the FEM analysis of infinite arrays: only one full-wave 3D-FEM simulation needs to be carried out independently of the scan angle and the array lattice dimensions, and this simulation does not require the imposition of periodic boundary conditions in opposite faces (avoiding the need for matching procedures).

To that effect, we first propose to use the frequency domain 3D-FEM combined with Modal Analysis to obtain the Generalized Scattering Matrix (GSM) in terms of spherical modes of a single, non-coupled, isolated antenna element [25], [7]. It is worth noting that this FEM step is independent of the infinite array arrangement where this antenna element will be placed, as no Floquet's theory is applied so far (i.e., the GSM is obtained for spherical modes, not Floquet modes). Therefore, this FEM simulation needs to be carried out only once, independent of the scan angle and the array lattice arrangement. From this GSM in terms of spherical modes, the response of the antenna element under desired infinite array conditions (i.e. by adjusting the lattice parameters and scan angle at this step) is computed by using translation of spherical modes based on addition theorems from every one of the surrounding elements. It is important to note that a limitation of the method, associated to the implementation based on addition theorems, is that the minimum spheres (or hemispheres on a ground plane) that circumscribe each one of the elements should not overlap [26]. The formulation, which involves the computation of lattice sums for spherical harmonics, is thoroughly derived. Although this postprocessing step needs to be performed at each scan angle, the computational speed-up factor overcomes traditional approaches, since it relies on analytical evaluations and computation of spherical harmonic lattice sums. Several methods have been developed for fast computation of lattice sums of spherical harmonics (see [27], [28] and references therein). Specifically, in this work we use the code provided in [29], [30], based on the exponentially convergent expressions provided in [31], [32] that use an extension of the Ewald summation procedure for 2D periodicity in 3D [33]. It should be noted that Ewald method has also been used previously to analyze periodic planar arrays of antennas or scatterers to accelerate the evaluation of Green Functions [34],[35],[20],[11]

II. Theory

A. Active reflection coefficient from the GSM of an isolated element.

A two-dimensional infinite periodic planar array of coupled antennas is considered. In the first step of the proposed analysis methodology, a single isolated antenna (i) of the array is characterized from its GSM. This GSM is obtained by applying a hybrid Finite Element/Modal Analysis method to a three-dimensional domain bounded by transmission line or waveguide feeding ports and a hemispherical port on a ground plane surrounding the antenna. This method has been detailed in [25] and [7]. The resulting GSM is given in terms of its submatrices as

$$\begin{bmatrix} \mathbf{\Gamma} & \mathbf{R} \\ \mathbf{T} & (\mathbf{S}-\mathbf{I}) \end{bmatrix} \begin{bmatrix} \mathbf{v}^{(i)} \\ \mathbf{a}^{(i)} \end{bmatrix} = \begin{bmatrix} \mathbf{w}^{(i)} \\ \mathbf{b}^{(i)} \end{bmatrix}, \tag{1}$$

where $\mathbf{v}^{(i)}$ and $\mathbf{w}^{(i)}$ are column vectors of complex amplitudes of incident and reflected modes on the feeding port of the antenna (i), $\mathbf{a}^{(i)}$ and $\mathbf{b}^{(i)}$ are column vectors of complex amplitudes of standing and scattered spherical modes on a spherical port, used to characterize the radiating region. Submatrices $\mathbf{\Gamma}$, $\mathbf{T}$, $\mathbf{R}$ and $\mathbf{S}$ are the reflection, transmission, reception, and scattering matrices of the isolated antenna, respectively, as defined in the classic theory [26], and $\mathbf{I}$ is the identity matrix.

The incident field on the spherical port of antenna (i) in the infinite coupled array is expressed as the superposition of the fields scattered by the rest of antenna elements, supposing no incoming field from outside the array. By expanding these fields in terms of spherical modes, the scattered field from antenna (k) can be expressed as an incident field in antenna (i), in terms of complex amplitudes of spherical modes, $\mathbf{b}^{(k)}$ and $\mathbf{a}^{(i)}$, respectively. In this way, these amplitudes are related as follows:

$$\mathbf{a}^{(i)} = \sum_{\substack{k=1 \\ k\neq i}}^{\infty} \mathbf{G}^{(i)(k)} \mathbf{b}^{(k)}, \tag{2}$$

where $\mathbf{G}^{(i)(k)}$ is the general translational matrix between antennas (i) and (k) for spherical modes, whose elements can be found in [36], or in an alternative way in [26]. By substituting (2) into (1) and assuming no incoming field from outside the array, two equations are obtained:

$$\mathbf{\Gamma v}^{(i)} + \mathbf{R}\sum_{\substack{k=1\\k\neq i}}^{\infty}\mathbf{G}^{(i)(k)}\mathbf{b}^{(k)} = \mathbf{w}^{(i)} \quad (3)$$

$$\mathbf{T} + (\mathbf{S}-\mathbf{I})\sum_{\substack{k=1\\k\neq i}}^{\infty}\mathbf{G}^{(i)(k)}\mathbf{b}^{(k)} = \mathbf{b}^{(i)}. \quad (4)$$

The transmission behavior of each antenna in the presence of the others in an infinite periodic array is identical for all the antennas Therefore, in an infinite array environment the following expression can be written for the complex amplitudes $\mathbf{b}^{(k)}$

$$\mathbf{b}^{(k)} = \mathbf{T}_{\text{Inf}}\mathbf{v}^{(k)}, \quad (5)$$

where $\mathbf{T}_{\text{Inf}}$ is the transmission matrix of each antenna in presence of the rest of elements in the array. Inserting (5) into (4), the latter results in

$$\mathbf{T v}^{(i)} + (\mathbf{S}-\mathbf{I})\sum_{\substack{k=1\\k\neq i}}^{\infty}\mathbf{G}^{(i)(k)}\mathbf{T}_{\text{Inf}}\mathbf{v}^{(k)} = \mathbf{T}_{\text{Inf}}\mathbf{v}^{(i)}. \quad (6)$$

Next, an excitation $\mathbf{v}^{(k)}$ over the infinite array, in order to scan the radiated field at a particular direction (θ_o, φ_o), is considered:

$$\mathbf{v}^{(k)} = \mathbf{v}e^{-\mathrm{j}\boldsymbol{\kappa_o}\cdot\boldsymbol{r}_k}, \quad (7)$$

where $\boldsymbol{\kappa_0} = \kappa(\sin\theta_0\cos\varphi_0\,\hat{x} + \sin\theta_0\sin\varphi_0\hat{y} + \cos\theta_0\hat{z})$, κ is the wavenumber in free space, $\boldsymbol{r}_k = x_k\hat{x} + y_k\hat{y}$ is the position vector of the antenna (k) and $\mathbf{v} = \mathbf{v}^{(i)}$ if antenna (i) is located at the origin of the coordinate system. Now, by using the excitation (7) into (6),

$$\mathbf{T v} + (\mathbf{S}-\mathbf{I})\sum_{\substack{k=1\\k\neq i}}^{\infty}\mathbf{G}^{(i)(k)}\mathbf{T}_{\text{Inf}}\mathbf{v}e^{-\mathrm{j}\boldsymbol{\kappa_o}\cdot\boldsymbol{r}_k} = \mathbf{T}_{\text{Inf}}\mathbf{v}. \quad (8)$$

$\boldsymbol{\Omega}(\boldsymbol{\kappa_o})$ has been defined in [37] as the matrix that designates the quasi-periodic lattice sum of the general translational matrices for spherical modes $\mathbf{G}^{(i)(k)}$

$$\boldsymbol{\Omega}(\boldsymbol{\kappa_o}) = \sum_{\substack{k=1\\k\neq i}}^{\infty}\mathbf{G}^{(i)(k)}e^{-\mathrm{j}\boldsymbol{\kappa_o}\cdot\boldsymbol{r}_k}. \quad (9)$$

It has been used in that work for modeling gratings composed of periodic arrays of identical discrete particles. This definition leads to the transmission matrix $\mathbf{T}_{\text{Inf}}(\boldsymbol{\kappa_o})$, particularized at (θ_o, φ_o)

$$\mathbf{T}_{\text{Inf}}(\boldsymbol{\kappa_o}) = [\mathbf{I} - (\mathbf{S}-\mathbf{I})\boldsymbol{\Omega}(\boldsymbol{\kappa_o})]^{-1}\mathbf{T}. \quad (10)$$

The reflection performance for an antenna in the array can be expressed similarly in terms of (9) and (10). Substituting (5) into (3) and taking into account the excitation in (7), the following expression is obtained

$$\mathbf{\Gamma v} + \mathbf{R}\sum_{\substack{k=1\\k\neq i}}^{\infty}\mathbf{G}^{(i)(k)}\mathbf{T}_{\text{Inf}}\mathbf{v}e^{-\mathrm{j}\boldsymbol{\kappa_o}\cdot\boldsymbol{r}_k} = \mathbf{w} \quad (11)$$

which, using the definition of $\boldsymbol{\Omega}(\boldsymbol{\kappa_o})$ in (9), results in

$$\mathbf{\Gamma v} + \mathbf{R}\,\boldsymbol{\Omega}(\boldsymbol{\kappa_o})\mathbf{T}_{\text{Inf}}(\boldsymbol{\kappa_o})\mathbf{v} = \mathbf{w}. \quad (12)$$

Finally, from (12), and considering the excitation modes in $\mathbf{v}$ and $\mathbf{w}$, the active reflection coefficient at the scan angle (θ_o, φ_o) is determined:

$$\mathbf{\Gamma}_a(\theta_o, \varphi_o) = \mathbf{\Gamma} + \mathbf{R}\,\boldsymbol{\Omega}(\boldsymbol{\kappa_o})\mathbf{T}_{\text{Inf}}(\boldsymbol{\kappa_o}). \quad (13)$$

It should be noted that the mathematical operations in (10) and (13) involve matrix multiplications and solving a linear system of dimension equal to the number of spherical modes required to describe the radiated field in the spherical port of the isolated element in (1). This number is chosen according to the criteria given in [38]

$$n = \left[\kappa r_{min} + 0.045\sqrt[3]{\kappa r_{min}}\,(-Ptr)\right],$$

where n is the degree of the spherical modes, r_{min} is the radius of the minimum sphere enclosing the element and P_{tr} is the relative truncated (i.e. excluded) power in dB with respect to the total radiated power due to the series truncation. We have checked that P_{tr} = -65 dB provides accurate results [39], so that, for a typical array element size of 0.4λ-0.7λ, n is not greater than 6, which leads to, at most, 48 spherical modes for elements on a ground plane. Convergence is absolute when increasing the degree n in the sense that, as the degree is increased, the precision of the calculated GSM is continuously improved. However, when the degree n is increased from an initial value chosen with the criterion that P_{tr} = -65 dB, this provides variations less than 10^{-5} for the GSM elements. Thus, a low computational effort will be required in this process since, although expression (9) must be computed for each scan angle, it requires a negligible time, as will be shown in Section III. The most time-consuming computation of the proposed procedure will be focused on the calculation of the GSM of the isolated element, given by (1), with FEM. Nevertheless, this effort is made only once, whatever the number of considered scan angles or array lattice arrangement.

B. Quasi-periodic lattice sum of the general translational matrices for spherical modes

As shown in [36], each element of matrix $\mathbf{G}^{(i)(k)}$ can be expressed as

$$G_{\mu\nu}^{mn} = \sum_p C(m,n,\mu,\nu)h_p(\kappa r_k)Y_p^{m-\mu}(\theta_k,\varphi_k), \quad (14)$$

where m and μ are the order, and n and ν are the degree, of the spherical modes referred to elements (i) and (k), respectively. Index p is related to n and ν, where the sum over the indices (n,ν) is finite. In (14), h_p is the spherical Hankel function for outward propagation, $Y_p^{m-\mu}$ is the scalar spherical harmonic, and $(r_k, \theta_k, \varphi_k)$ are the spherical coordinates of element (k) with respect to element (i). Formulae for the computation of C based on addition theorems have been reported in many works but for the first time in [36], although there is a well-documented sign error in that paper [40], [41]. Additional

details on spherical modes and the use of the addition theorems as well as many complementary references on this can be found in [42]

Consequently, each element of $\boldsymbol{\Omega}(\boldsymbol{\kappa_o})$ can be written as [37]

$$\Omega_{\mu\nu}^{mn} = \sum_p C(m,n,\mu,\nu) \sum_{\substack{k=1 \\ k\neq i}}^{\infty} h_p(\kappa r_k) Y_p^{m-\mu}(\theta_k,\varphi_k) e^{-\mathrm{j}\boldsymbol{\kappa_o}\cdot\mathbf{r}_k} \quad (15)$$

so that

$$\Omega_{\mu\nu}^{mn} = \sum_p C(m,n,\mu,\nu) ls(m-\mu,p), \quad (16)$$

where the term

$$ls(m-\mu,p) = \sum_{\substack{k=1 \\ k\neq i}}^{\infty} h_p(\kappa r_k) Y_p^{m-\mu}(\theta_k,\varphi_k) e^{-\mathrm{j}\boldsymbol{\kappa_o}\cdot\mathbf{r}_k} \quad (17)$$

accounts for the lattice sums. As already mentioned above, the code from [29], provided in [30], is used in this work for the efficient computation of (17).

C. Active (embedded) element pattern computation

As shown in [7], the radiated field of an array in terms of spherical modes is computed as follows

$$\vec{\mathrm{E}}_{rad}(r,\theta,\varphi) = \frac{e^{-\mathrm{j}\kappa r}}{\kappa r} \sum_{k=0}^{\infty} \mathbf{e}(\theta,\varphi)\, \mathbf{b}^{(k)}\, \mathrm{e}^{\mathrm{j}\boldsymbol{\kappa}\cdot\mathbf{r}_k}, \quad (18)$$

where $\mathbf{e}(\theta,\varphi)$ is a row vector with the expressions of the far-field modes [26], $\mathbf{b}^{(k)}$ is a column vector with the corresponding complex amplitudes for antenna (k), and $\boldsymbol{\kappa} = \kappa(\sin\theta\cos\varphi\,\hat{x} + \sin\theta\sin\varphi\,\hat{y} + \cos\theta\hat{z})$. For an infinite array pointing at a particular direction (θ_o,φ_o), amplitudes $\mathbf{b}^{(k)}$ are obtained by using the excitation (7) in (5)

$$\mathbf{b}^{(k)} = e^{-\mathrm{j}\boldsymbol{\kappa_o}\cdot\mathbf{r}_k}\mathbf{T}_{\mathrm{Inf}}\mathbf{v}. \quad (19)$$

Now, by introducing (19) into (18), we obtain

$$\vec{\mathrm{E}}_{rad}(r,\theta=\theta_o,\varphi=\varphi_o) = \frac{e^{-\mathrm{j}\kappa r}}{\kappa r} \sum_{k=0}^{\infty} \mathbf{e}(\theta,\varphi) e^{\mathrm{j}(\boldsymbol{\kappa}-\boldsymbol{\kappa_o})\cdot\mathbf{r}_k} \mathbf{T}_{\mathrm{Inf}}\mathbf{v}\big|_{\theta=\theta_o,\varphi=\varphi_o}. \quad (20)$$

Identifying in this expression the array factor of the infinite array scanned to (θ_o,φ_o), $\mathbf{AF}(\theta,\varphi) = \sum_{k=0}^{\infty} e^{\mathrm{j}(\boldsymbol{\kappa}-\boldsymbol{\kappa_o})\cdot\mathbf{r}_k}$, (20) results in the following:

$$\vec{\mathrm{E}}_{rad}(r,\theta=\theta_o,\varphi=\varphi_o) = \frac{e^{-\mathrm{j}\kappa r}}{\kappa r} \mathbf{AF}(\theta,\varphi)\mathbf{e}(\theta,\varphi)\mathbf{T}_{\mathrm{Inf}}\mathbf{v}\big|_{\theta=\theta_o,\varphi=\varphi_o}. \quad (21)$$

Since (19) is only valid for a particular direction (θ_o,φ_o), then

$$\vec{\mathrm{E}}_{rad}(r,\theta_o,\varphi_o) = \frac{e^{-\mathrm{j}\kappa r}}{\kappa r} \mathbf{AF}(\theta_o,\varphi_o)\mathbf{e}(\theta_o,\varphi_o)\mathbf{T}_{\mathrm{Inf}}\mathbf{v}. \quad (22)$$

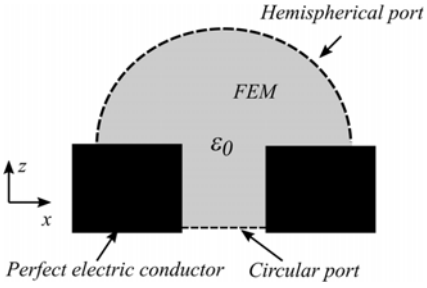

Fig. 1. Side view of the isolated aperture. Shaded region: analyzed with FEM.

On the other hand, the radiated field $\vec{\mathrm{E}}_{rad}$ can also be expressed as the superposition of the active element field pattern $\vec{\mathrm{E}}_{ae}(\theta,\varphi)$ and the array factor

$$\vec{\mathrm{E}}_{rad}(r,\theta,\varphi) = \frac{e^{-\mathrm{j}\kappa r}}{\kappa r} \mathbf{AF}(\theta,\varphi)\vec{\mathrm{E}}_{ae}(\theta,\varphi)\mathbf{v}. \quad (23)$$

Finally, by comparing (22) and (23), the active element field pattern for a given scan angle can be analytically obtained from $\mathbf{T}(\boldsymbol{\kappa_o})$ as follows:

$$\vec{\mathrm{E}}_{ae}(\theta_o,\varphi_o) = \mathbf{e}(\theta_o,\varphi_o)\mathbf{T}_{\mathrm{Inf}}(\boldsymbol{\kappa_o}). \quad (24)$$

This expression is also obtained with a low computational effort as well as the active reflection coefficient given by (13).

III. Results

In this section, three different infinite arrays are analyzed to show the capabilities of the proposed method. The results are compared with other numerical predictions available in the literature in order to evaluate its accuracy.

A. Infinite array of circular apertures on a triangular lattice

The first example consists of an array of empty circular waveguide apertures in a ground plane arranged on an equilateral triangular grid, previously analyzed in [43]. Fig. 1 shows the side view of the isolated element as studied with FEM. The geometry and dimensions of the array are depicted in Fig. 2. The computed active reflection coefficient magnitude in E and H-planes compared with the results in the reference are shown in Figs. 2 and 3, respectively. A very good agreement is observed in both cases. Fig. 4 shows the active element field pattern, not reported in the reference, in both planes.

Regarding the computational effort, the aperture diameter of the array element, 0.68λ, determines a number of spherical modes equal to 48, required to describe the radiated field in (1). Thus, computation of (9) to calculate the quasi-periodic lattice sum of the general translational matrices only takes 0.0007 seconds per scan angle on a personal laptop (i7-9850H). The computation of (13) and (24) to obtain the active reflection coefficient and the active element pattern only requires operations with matrices of dimension equal to 48 and solving a linear system of the same size. As stated in section II, the main computational cost is employed in the computation of the GSM of the isolated element (1) with FEM that in this case takes 10 seconds.

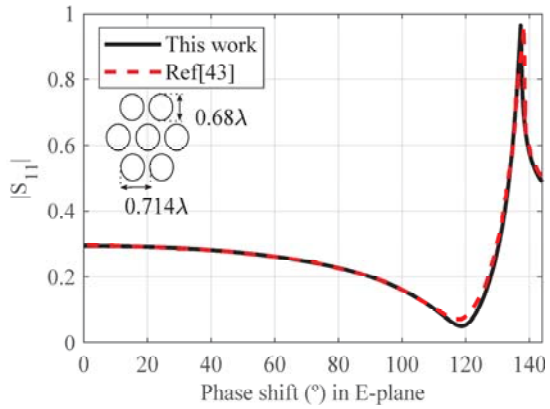

Fig. 2. Active reflection coefficient magnitude versus the phase shift of the infinite array of circular apertures depicted inside the figure. E-plane scan.

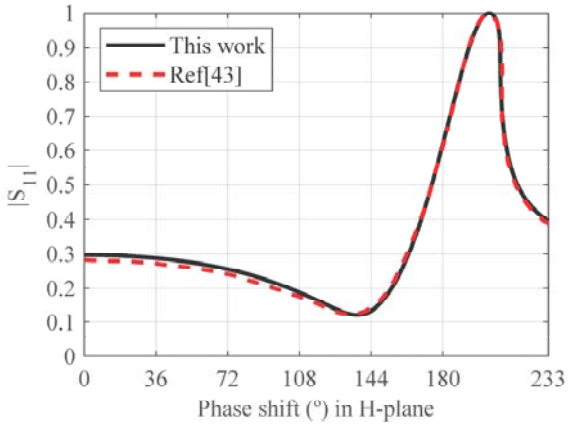

Fig. 3. Active reflection coefficient magnitude versus the phase shift of the infinite array of circular apertures given inside Fig. 2. H-plane scan.

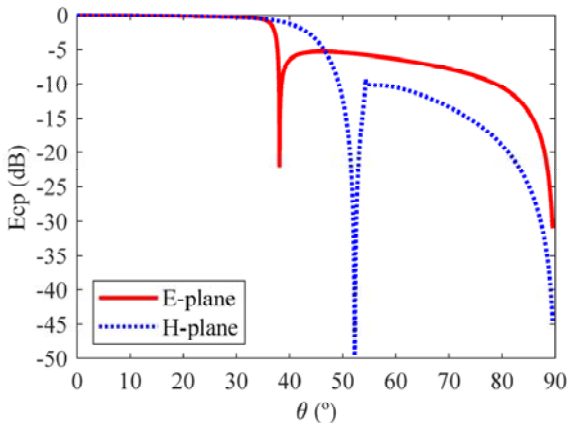

Fig. 4. Active element field pattern of the infinite array of circular apertures depicted inside Fig.2.

B. Infinite array of cavity-backed square patch antennas with coaxial probe feeding

An infinite array of probe-fed cavity-backed square patch antennas on a square lattice is now considered. Results are compared with those obtained with a full wave Finite Element/Floquet-based method (FEM/Floquet) [15] and those given in [7] using a Mode Matching method (MM) [44]. Fig. 5 shows the side view of the isolated element as studied with FEM. The geometry of the array in a 2x2 subarray is depicted in Fig. 6.

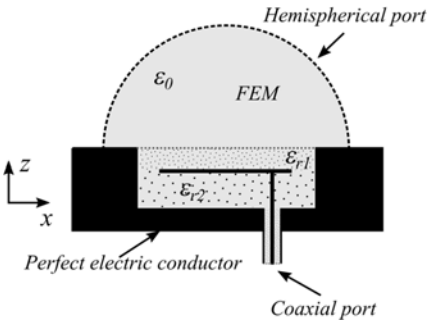

Fig. 5. Side view of the isolated probe-fed cavity-backed square patch antenna. Shaded region: analyzed with FEM.

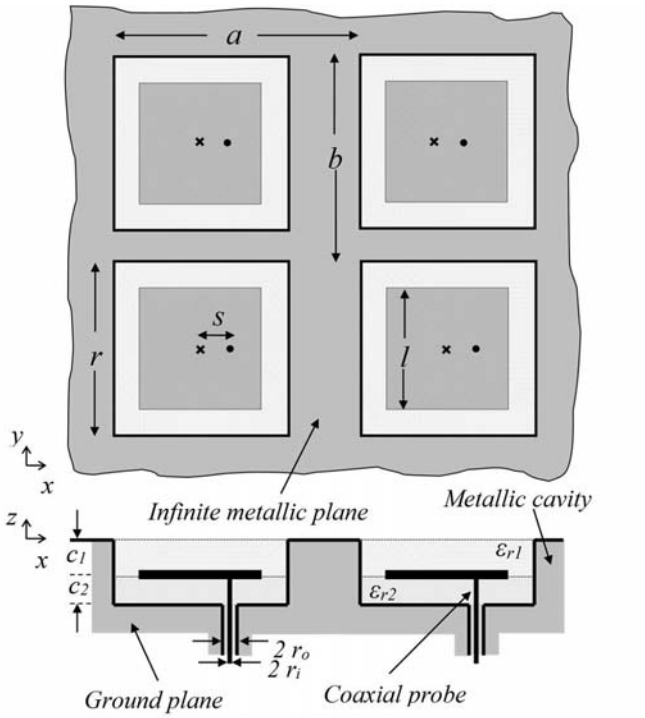

Fig. 6. Infinite array of coaxial probe-fed cavity-backed patch antennas. Top and side view of a 2x2 array is shown. l = 1.35 cm, r = 1.815 cm, c_2 = 2.42 mm, c_1 = 2.9 mm, s = 1.7 mm, ε_2 = 2.62, ε_1 = 1.0. Coaxial feed (SMA connector): ε_{rx} = 1.951, r_i = 0.65 mm, r_o = 2.05 mm.

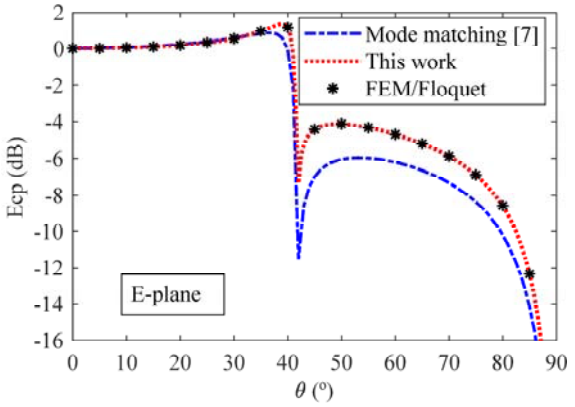

Fig. 7. Active element field pattern in E-plane of the infinite array of cavity-backed patch antennas defined in Fig. 6.

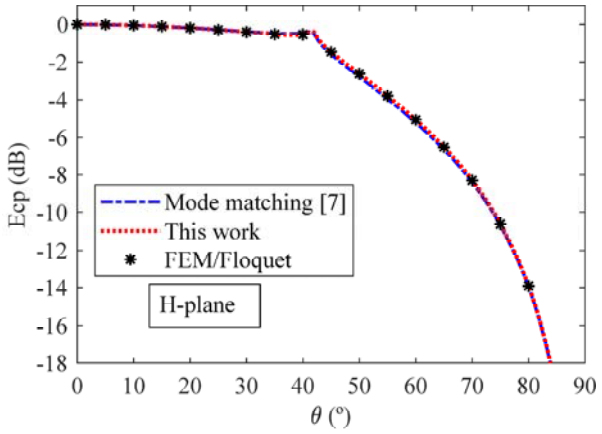

Fig. 8. Active element field pattern in H-plane of the infinite array of cavity-backed patch antennas defined in Fig. 6.

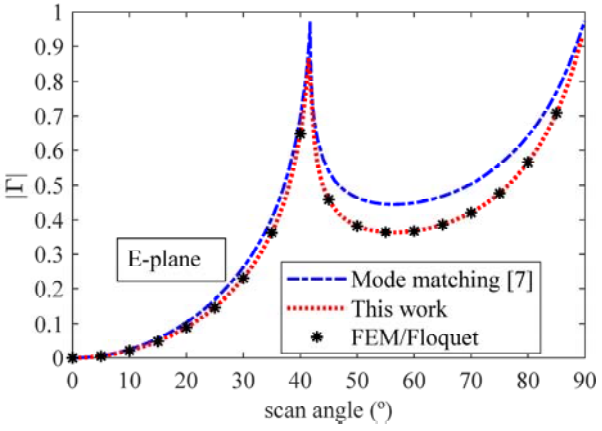

Fig. 9. Broadside-matched active reflection coefficient magnitude versus the scan angle in E-plane of the infinite array of cavity-backed patch antennas defined in Fig. 6.

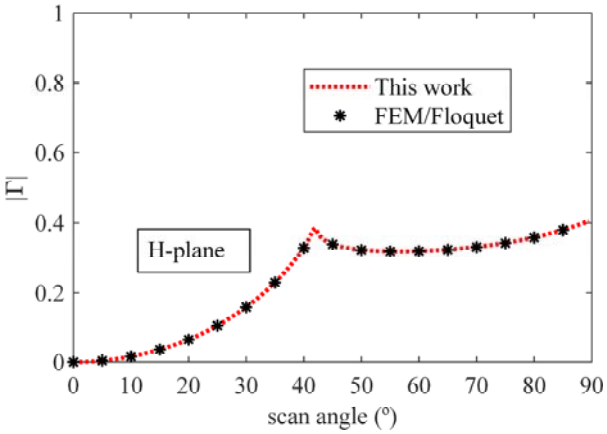

Fig. 10. Broadside-matched active reflection coefficient magnitude versus the scan angle in H-plane of the infinite array of cavity-backed patch antennas defined in Fig. 6.

Figs. 7 and 8 show the computed active element field pattern of the co-polarized component in E and H-planes, respectively, at 6 GHz for an element spacing a = b = 0.6λ. The results obtained with the proposed method show an excellent agreement in both planes with the FEM/Floquet analysis. However, the curve obtained from MM method deviates in E-plane from the scan blindness angle to the end-fire direction. This discrepancy may be due to the phenomenon of relative convergence when applying the MM method.

Figs. 9 and 10 show the broadside-matched active reflection coefficient magnitude versus the scan angle in E and H-planes respectively. An excellent agreement with the FEM/Floquet in both planes is also observed, whereas the curve obtained from the MM in E-plane shows a similar deviation as the observed for the active reflection coefficient.

In this example, the total CPU simulation time for the computation of (9) and (13) at 180 scan angles, in order to obtain the active reflection coefficient with the proposed method, is only 0.1 seconds. The computation of the GSM of the isolated element with FEM, for which only 24 spherical modes are required, takes 16 seconds. As stated in Section II, this last one is the most time-consuming step of the proposed procedure. On the other hand, in the characterization of the infinite array from the FEM/Floquet method in [15], the time required to perform the analysis at one scan angle is similar to the characterization of the isolated element in the proposed method. This comparison illustrates the considerable effort in computer time and memory requirements saved with the proposed analysis technique.

C. Infinite array of cylindrical dielectric resonator antennas with coaxial probe feeding

A square grid infinite array of probe-fed cylindrical dielectric resonator antennas (DRA´s) on a ground plane is analyzed in this last example. Fig. 11 shows the side view of the isolated element as studied with FEM. The geometry and dimensions of the array in a 2x2 subarray are shown in Fig. 12. The resonant

frequency of the isolated element, analyzed in [45], is 10 GHz. The element spacing of the array is chosen to be 0.5λ at 10 GHz.

Fig. 13 shows the computed active reflection coefficient as a function of frequency at two scan angles, 0º and 45º, in E-plane, compared with the results obtained with the FEM/Floquet analysis [15] and simulated with CST MWS [4]. An excellent agreement is found in all cases. The figure also shows the computed reflection coefficient versus frequency of the isolated element. In this figure it can be observed that the resonant frequency, at broadside scan angle, shifts 0.5 GHz with respect to resonant frequency of the isolated element. This effect has been previously reported in [46] for DRA antennas. In fact, the resonant frequency changes with the scan angle so that it becomes close to 10 GHz at 45º, as shown in Fig. 13.

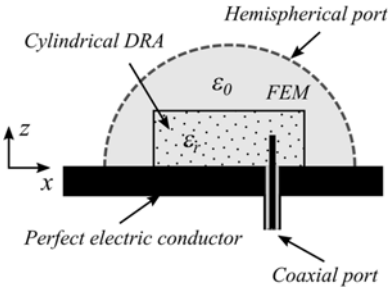

Fig. 11. Side view of the isolated cylindrical DRA. Shaded region: analyzed with FEM.

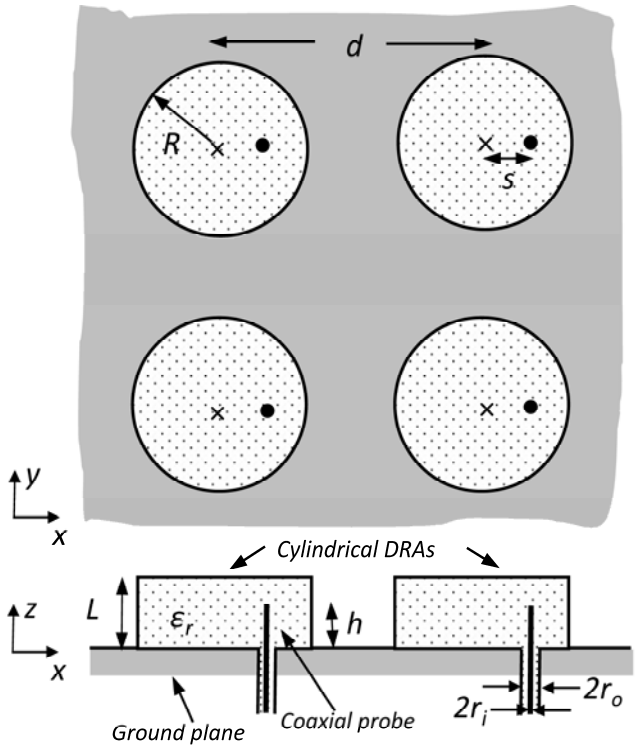

Fig. 12. Top and side view of a 2×2 finite array of cylindrical DRAs with coaxial probe feeding. R=4.2 cm, L=3 cm, ε_r=12, h= 2.4 cm, s=3.5 cm, d= 1.49896 cm. Coaxial feed: ε_{rx} =1, r_i=0.1 mm, r_o=0.2301 mm.

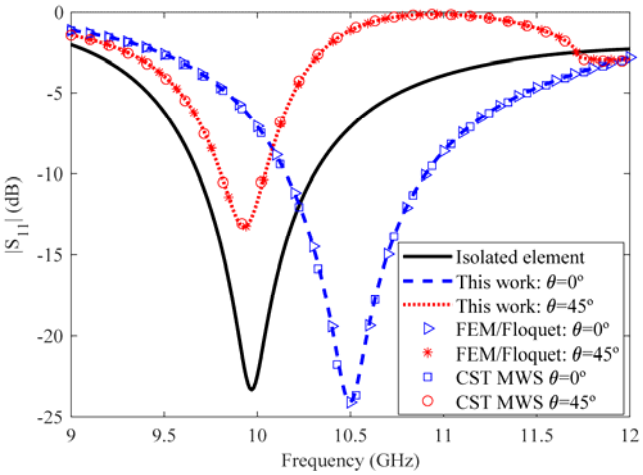

Fig. 13. Active reflection coefficient magnitude versus frequency of the infinite array of DRAs defined in Fig. 12 for θ = 0º and 45º scan angles in the E-plane, compared with the reflection coefficient of the isolated element.

For a wideband analysis of the infinite array, the method proposed here requires one FEM analysis per frequency of the isolated element, in the same way that the FEM/Floquet method for a fixed scan angle. However, the analysis of the isolated element for a wide band can also be performed more efficiently with a reliable fast frequency sweep based on a reduced basis method [47] whereas, as far as the authors know, no fast frequency sweep technique has been reported for FEM/Floquet method. In this work, we have used this reliable fast frequency method to compute 300 frequency points with a computational cost of 325 seconds, which corresponds with the computational effort of only 9 frequency points with the frequency-by-frequency FEM analysis, whereas the postprocessing to obtain the active reflection coefficient by computing (9) and (13) only takes 0.2 seconds for the whole band.

IV. Conclusion

A method for the efficient analysis of infinite periodic arrays of antennas based on the Finite Element Method, addition theorems for spherical modes and lattice sums has been presented. It has been shown that this method provides the same results as the classical FEM/Floquet for those arrays whose elements can be individually described by means of spherical modes and, due to the use of the addition theorems, that their minimum spheres do not overlap. However, with the proposed method the numerical effort is performed only once, whatever the scan angle or the lattice, whereas FEM/Floquet requires one numerical analysis per scan angle and lattice. Advantages of a reliable fast frequency sweep can also be exploited in this case.

References

[1] N. Amitay, V. Galindo, and C. P. Wu, *Theory and Analysis of Phased Array Antennas*. New York, NY, USA: Wiley, 1972.

[2] A. K. Bhattacharyya, *Phased Array Antennas*. Hoboken, NJ, USA: Wiley, 2006.

[3] Ansys HFSS 2022, Ansys Inc., Canonsburg, Pennsylvania, USA, 2022.

[4] CST Suite 2021, CST AG, Darmstadt, Germany, 2021.

[5] Altair Feko, Altair Inc., Troy, Michigan, USA, 2022.

[6] C. Craeye and D. González-Ovejero, "A review on mutual coupling analysis," *Radio Sci.*, vol. 46, no. 2, RS2012, Apr. 2011, doi: 10.1029/2010RS004518.

[7] J. Rubio, M. A. González, and J. Zapata, "Generalized-scattering-matrix analysis of a class of finite arrays of coupled antennas by using 3-D FEM and spherical mode expansion," *IEEE Trans. Antennas Propag.*, vol. 53, pp. 1133–1144, Mar. 2005, doi: 10.1109/TAP.2004.842687.

[8] T. Marinović, D. I. Z. de Villiers, D. J. Bekers, M. N. Johansson, A. Stjernman, R. Maaskant, and G. A. E. Vandenbosch, "Fast characterization of mutually coupled array antennas using isolated antenna far-field data," *IEEE Trans. Antennas Propag.*, vol. 69, no. 1, pp. 206-218, Jan. 2021, doi: 10.1109/TAP.2020.3016395.

[9] G. Floquet, "Sur les équations différentielles linéaires à coefficients périodiques," *Ann. Ecole Norm. Sér.,* vol. 12, pp. 47–88, 1883.

[10] X. Wang, D. H. Werner and J. P. Turpin, "Application of AIM and MBPE techniques to accelerate modeling of 3-D doubly periodic structures with nonorthogonal lattices composed of bianisotropic media," *IEEE Trans. Antennas Propag.*, vol. 62, no. 8, pp. 4067-4080, Aug. 2014, doi: 10.1109/TAP.2014.2322903.

[11] B.J. Morsink, G. H. C. van Werkhoven, A. G. Tijhuis, and S. W. Rienstra, "An accelerated coupled feed-radiator-frequency selective surface model for the next generation active phased array systems," in *IEEE Int. Symp. Phased Array Systems and Technology*, Oct. 2003, pp. 470-475.

[12] C. Wan and J. A. Encinar, "Efficient computation of generalized scattering matrix for analyzing multilayer periodic structures," *IEEE Trans. Antennas Propag.*, vol. 43, no. 11, pp. 1233-1242., Nov. 1995.

[13] S. Monni, G. Gerini, A. Neto, and A. G. Tijhuis, "Multimode equivalent networks for the design and analysis of frequency selective surfaces," *IEEE Trans. Antennas Propag.*, vol. 55, no. 10, pp. 2824-2835, Oct. 2007, doi: 10.1109/TAP.2007.905846.

[14] M. A. González de Aza, J.A. Encinar, J. Zapata, and M. Lambea, "Full-wave analysis of cavity-backed and probe-fed microstrip patch arrays by a hybrid mode-matching generalized scattering matrix and finite-element method," *IEEE Trans. Antennas Propag.*, vol. 46, no. 2, pp. 234-242, Feb. 1998.

[15] V. de la Rubia, J. Zapata and M. A. Gonzalez, "Finite element analysis of periodic structures without constrained meshes," *IEEE Trans. Antennas Propag.*, vol. 56, no. 9, pp. 3020-3028, Sept. 2008, doi: 10.1109/TAP.2008.928776.

[16] J.M. Jin, Z. Lou, Y. J. Li, N. Riley, and D. Riley, "Finite element analysis of complex antennas and arrays," *IEEE Trans. Antennas Propag.*, vol. 56, no. 8, pp. 2222–2240, Aug. 2008, doi: 10.1109/TAP.2008.926776.

[17] J.M. Jin and J. L. Volakis, "Scattering and radiation analysis of three-dimensional cavity arrays via a hybrid finite-element method," *IEEE Trans. Antennas Propag.*, vol. 41, no. 11, pp. 1580-1586, Nov. 1993, doi: 10.1109/8.267360.

[18] D. T. McGrath and V. P. Pyati, "Phased array antenna analysis with the hybrid finite element method," *IEEE Trans. Antennas Propag.*, vol. 42, no. 12, pp. 1625-1630, Dec. 1994, doi: 10.1109/8.362811.

[19] E. W. Lucas and T. P. Fontana, "A 3-D hybrid finite element/boundary element method for the unified radiation and scattering analysis of general infinite periodic arrays," *IEEE Trans. Antennas Propag.*, vol. 43, no. 2, pp. 145-153, Feb. 1995, doi: 10.1109/8.366376.

[20] T. F. Eibert, J. L. Volakis, D. R. Wilton, and D. R. Jackson, "Hybrid FE/BI modeling of 3-D doubly periodic structures utilizing triangular prismatic elements and an MPIE formulation accelerated by the Ewald transformation," *IEEE Trans. Antennas Propag.*, vol. 47, no. 5, pp. 843–850, May 1999, doi: 10.1109/8.774139.

[21] M. N. Vouvakis, Z. Cendes, and J.-F. Lee, "A FEM domain decomposition method for photonic and electromagnetic band gap structures," *IEEE Trans. Antennas Propag.*, vol. 54, no. 2, pp. 721–733, Feb. 2006, doi: 10.1109/TAP.2005.863095.

[22] M. N. Vouvakis, K. Zhao, and J.-F. Lee, "Finite-element analysis of infinite periodic structures with nonmatching triangulations," *IEEE Trans. Magn.*, vol. 42, no. 4, pp. 691–694, Apr. 2006, doi: 10.1109/TMAG.2006.872483.

[23] R. Chiniard, A. Barka and O. Pascal, "Hybrid FEM/Floquet modes/PO technique for multi-incidence RCS prediction of array antennas," *IEEE Trans. Antennas Propag.*, vol. 56, no. 6, pp. 1679-1686, Jun. 2008, doi: 10.1109/TAP.2008.923328.

[24] J. B. Manges, J. W. Silvestro, and R. Petersson, "Accurate and efficient extraction of antenna array performance from numerical unit-cell data," in *2011 41st European Microwave Conf.*, Oct. 2011, pp. 1019-1022, doi: 10.23919/EuMC.2011.6101726.

[25] J. Rubio, M. A. González and J. Zapata, "Analysis of cavity-backed microstrip antennas by a 3-D finite element/segmentation method and a matrix Lanczos-Pade algorithm (SFELP)," *IEEE Antennas Wireless Propag. Lett.*, vol. 1, no.1, pp. 193-195, 2002, doi: 10.1109/LAWP.2002.807783.

[26] J. E. Hansen, Ed., *Spherical Near-Field Antenna Measurements*. London, U.K.: Peter Peregrinus Ltd., 1988.

[27] C. M. Linton, "Lattice sums for the Helmholtz equation," *SIAM Rev.*,vol. 52, no. 4, pp. 630–674, Jan. 2010, doi: 10.1137/09075130X.

[28] C. M. Linton, I. Thompson, "One- and two-dimensional lattice sums for the three-dimensional Helmholtz equation," *J. Comput. Phys.*, vol. 228, no. 6, pp. 1815-1829, 2009, doi: 10.1016/j.jcp.2008.11.013.

[29] J. B. Pendry, *Low Energy Electron Diffraction*. London, UK: Academic Press, 1974.

[30] A. Moroz, "Welcome to Wave Scattering", http://wave-scattering.com (accessed Feb. 18, 2022).

[31] K. Kambe, "Theory of Electron Diffraction by Crystals. Green's function and integral equation," *Z. Naturforschg. A*, vol. 22a, no. 4, pp. 422-431, 1967, doi: 10.1515/zna-1967-0402.

[32] K. Kambe, "Theory of Low-Energy Electron Diffraction. I. Application of the cellular method to monoatomic layers," *Z. Naturforschg. A*, vol. 22a, no. 3, pp. 322-330, 1967, doi: 10.1515/zna-1967-0305.

[33] A. Moroz, "Quasi-periodic Green's functions of the Helmholtz and Laplace equations", *J. Phys. A: Math. Gen.*, vol. 39, no. 36, Aug. 2006, doi: 10.1088/0305-4470/39/36/009.

[34] K. E. Jordan, G. R. Richter, and P. Sheng, "An efficient numerical evaluation of the Green's function for the Helmholtz operator on periodic structures," *Journal Comput. Phys.*, vol. 63, no. 1, pp. 222-235, Mar. 1986, doi: 10.1016/0021-9991(86)90093-8.

[35] I. Stevanovic, P. Crespo-Valero, K. Blagovic, F. Bongard, and J. R. Mosig, "Integral-equation analysis of 3-D metallic objects arranged in 2-D lattices using the Ewald transformation," *IEEE Trans. Microw. Theory Techn.*, vol. 54, no. 10, pp. 3688-3697, Oct. 2006, doi: 10.1109/TMTT.2006.882876.

[36] O. R. Cruzan, "Translational Addition theorem for spherical vector wave functions," *Q. Appl. Math*, vol. 20, no. 1, pp. 33-40, Apr. 1962, doi: 10.1090/qam/132851.

[37] B. Stout, "Spherical harmonic Lattice Sums for Gratings", in *Gratings: Theory and Numeric Applications*, E. Popov, Ed., Institut Fresnel, PUP, Marsille, France: 2012.

[38] F. Jensen and A. Frandsen, "On the number of modes in spherical wave expansions," in Proc. 26th AMTA, Stone Mountain Park, GA, USA, Oct. 17–22, 2004, pp. 489–494.

[39] J. Rubio, A. Gómez García, R. Gómez Alcalá, J. García, Y. Campos-Roca, "Simultaneous use of addition theorems for cylindrical and spherical waves for the fast full-wave analysis of SIW-based antenna arrays," *IEEE Trans. Antennas Propag.*, vol. 67, no. 12, pp. 7379-7386, Dec. 2019, doi: 10.1109/TAP.2019.2930175.

[40] L. Tsang, J.A. Kong, "Effective propagation constants for coherent electromagnetic wave propagation in media embedded with dielectric scatters," *J. Appl. Phys.* vol. 11, no. 53, pp. 7162–7173, 1982, doi: 10.1063/1.331611.

[41] P. C. Waterman, N.E. Pedersen, "Electromagnetic scattering by periodic arrays of particles," *J. Appl. Phys.*, vol. 8, no. 59, pp. 2609–2618, 1986, doi: 10.163/1.336988.

[42] M. I. Mishchenko, L. D. Travis, and A. A. Lacis, *Scattering, absorption, and emission of light by small particles*. Cambridge, UK: Cambridge University Press, 2002.

[43] N. Amitay and V. Galindo, "Characteristics of dielectric loaded and covered circular waveguide phased arrays", *IEEE Trans. Antennas Propag.*, vol. 17, no. 6, pp. 722–729, Nov. 1969, doi: 10.1109/TAP.1969.1139551.

[44] M. A. González, J. A. Encinar, and J. Zapata, "Radiation pattern computation of cavity-backed and probe-fed stacked microstrip patch arrays," *IEEE Trans. Antennas Propag.*, vol. 48, no. 4, pp. 502–509, Apr. 2000, doi: 10.1109/8.843663.

[45] R. Chair, A. A. Kishk and Kai-Fong Lee, "Comparative study on the mutual coupling between different sized cylindrical dielectric resonators antennas and circular microstrip patch antennas," *IEEE Trans. Antennas Propag.*, vol. 53, no. 3, pp. 1011-1019, Mar. 2005, doi: 10.1109/TAP.2004.842682.

[46] A. Motevasselian, A. Ellgardt and B. L. G. Jonsson, "A comparison of a finite and an infinite antenna array with cylindrical dielectric resonator elements," *2011 XXXth URSI General Assembly and Scientific Symposium*, 2011, pp. 1-4, doi: 10.1109/URSIGASS.2011.6050307

[47] V. de la Rubia, U. Razafison and Y. Maday, "Reliable fast frequency sweep for microwave devices via the reduced-basis method," *IEEE Trans. Microw. Theory Techn.*, vol. 57, no. 12, pp. 2923-2937, Dec. 2009, doi: 10.1109/TMTT.2009.2034208.

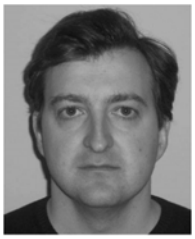

Jesús Rubio was born in Talavera de la Reina, Toledo, Spain. He received the M.S. and Ph.D. degrees in telecommunication engineering from the Universidad Politécnica de Madrid, Madrid, Spain, in 1995 and 1998, respectively.

Since 1994, he has been collaborating with the Departamento de Electromagnetismo y Teoría de Circuitos, Universidad Politécnica de Madrid. He is currently working with the Departamento de Tecnología de Computadores y Comunicaciones, Universidad de Extremadura, as a Professor. His current research interests include application of the finite element method and modal analysis to passive microwave circuits problems and antennas.

Miguel A. González de Aza was born in Madrid, Spain. He received the Ingeniero de Telecomunicación and Ph.D. degrees from the Universidad Politécnica de Madrid (UPM), Madrid, Spain, in 1989 and 1997, respectively.

Since 1990, he has been with the Escuela Técnica Superior de Ingenieros de Telecomunicación, Universidad Politécnica de Madrid, first as a Research Assistant, as an Assistant Professor from 1992 to 1997 and an Associate Professor in 1997. His current research interests include analytical and numerical techniques for the analysis and design of antennas, arrays of antennas and microwave passive circuits.

Juan Córcoles was born in Albacete, Spain, in 1981.

He received the Ingeniero de Telecomunicación degree (the B.Sc. and M.Sc. degrees in electrical engineering) and the Doctor Ingeniero de Telecomunicación degree (the Ph.D. degree in electrical engineering) from the Universidad Politécnica de Madrid, Spain, in 2004 and 2009, respectively, the Diplomado en Ciencias Empresariales degree (the B.Sc. degree in business science) from the Universidad Complutense de Madrid, in 2008, and the Licenciado en Economía degree (the M.Sc. degree in Economics) from the Universidad Nacional de Educación a Distancia, Madrid, Spain, in 2010.

He was a Visiting Researcher with the Institut für Hochfrequenztechnik und Elektronik (IHE), Universität Karlsruhe (TH), Germany, from November 2008 to March 2009, IT'IS Foundation, ETHZ, Zurich, Switzerland, from July 2013 to September 2013 and June 2016 and August 2016, and King's College London, U.K., from October 2018 to December 2018.

Since 2010, he has been with the Universidad Autónoma de Madrid, Spain, where he became an Associate Professor, in 2015.

His current research interests include the development and application of computational methods and optimization techniques to the analysis and design of microwave circuits and antennas, especially antenna arrays, as well as medical and other novel applications of radiofrequency electromagnetic fields.

Rafael Gómez Alcalá (M'01) was born in Córdoba, Spain. He received the degree in telecommunication engineering and the Ph.D. degree in telecommunication from the University of Vigo, Pontevedra, Spain, in 1990 and 1996, respectively.

In 1999, he moved to the University of Extremadura, Cáceres, Spain, where he is currently a Faculty Member of the Polytechnic School of Cáceres. His research interests include microwave filters and antenna design.